Microwave-induced flow of vortices in long Josephson junctions

F. L. Barkov*, M. V. Fistul† and A. V. Ustinov
Physikalisches Institut III, Universität Erlangen-Nürnberg, D-91058, Erlangen, Germany
(Dated: February 2, 2008)

We report experimental and numerical study of microwave-induced flow of vortices in long Josephson junctions at zero dc magnetic field. Our intriguing observation is that applying an ac-bias of a small frequency $f \ll f_p$ and sufficiently large amplitude changes the current-voltage characteristics (I-V curve) of the junction in a way similar to the effect of dc magnetic field, well known as the flux-flow behavior. The characteristic voltage V of this low voltage branch increases with the power P of microwave radiation as $V_s \propto P^{\alpha}$ with the index $\alpha \simeq 0.5$. Experiments using a low-temperature laser scanning microscope unambiguously indicate the motion of Josephson vortices driven by microwaves. Numerical simulations agree with the experimental data and show strongly *irregular* vortex motion. We explain our results by exploiting an analogy between the microwave-induced vortex flow in long Josephson junctions and incoherent multi-photon absorption in small Josephson junctions in the presence of large thermal fluctuations. In the case of long Josephson junctions the spatially-temporal chaos in the vortex motion mimics the thermal fluctuations. In accordance with this analogy, a control of the intensity of chaos in a long junction by changing its damping constant leads to a pronounced change in the shape of the I-V curve. Our results provide a possible explanation to previously measured but not yet understood microwave-driven properties of intrinsic Josephson junctions in high-temperature superconductors.

PACS numbers: 74.50.+r; 74.25.-Nf; 85.25.Cp

I. INTRODUCTION

The discovery of intrinsic Josephson junctions in highly anisotropic high-T_c superconductors [1] has boosted the interest in the dynamics of Josephson vortices. These junctions were proposed as candidates for high power flux-flow oscillators at THz frequencies. The Josephson penetration depth $\lambda_{\rm J}$ in these junctions is rather small, typically of the order of $0.1\,\mu$m. Thus the standard micron-size intrinsic junctions possess motion of Josephson vortices, similarly to conventional low-T_c long ($\ell \gg \lambda_J$) junctions.

Many of the experiments with intrinsic junctions have been performed during the last decade at microwave (GHz) frequencies, which are well below the junction's zero-bias plasma frequency $f_{\rm p}$. These experiments led to observations of Josephson plasma resonance [2] and novel microwave-induced branches in the current-voltage characteristics (I-V curves) of intrinsic junctions [3]. While the Josephson plasma resonance has been thoroughly investigated and explained, the effects produced by microwaves on I-V curves have not yet been fully understood. One obvious reason for that is that the dynamics of Josephson junctions at frequencies $f < f_{\rm p}$ can be chaotic and thus complicated. Nonetheless, many experiments with underdamped intrinsic junctions driven by microwaves at zero dc magnetic field revealed very puzzling *smooth branches* in I-V curves [3]. The aim of our work is to find an explanation for this behavior. For this purpose, we have performed a detailed study of conventional low-T_c long Josephson junctions under strong microwave irradiation and have done also numerical simulations, which we compare with experimental data.

The dynamics of long Josephson junctions under microwave irradiation was studied in various contexts in the past both theoretically and experimentally. In particular, there had been an extensive search for regimes in vortex motion synchronized by the external microwaves [4]. The vortex dynamics in underdamped junctions under the influence of ac drive is often very complicated, showing along with synchronized (phase-locked) dynamics [5] also the chaotic behavior [6]. The spatially-temporal chaos in underdamped long Josephson junctions typically occurs at low drive frequencies ($f < f_{\rm p}$). Moreover, the chaotic behavior in long junctions may appear even in the absence of external irradiation at low characteristic frequencies of vortex oscillations [7]. Increase of damping usually helps obtaining more regular dynamics.

The interest to drive vortices in long junctions by microwaves has been also biased by practical applications. Recently, low-frequency microwave properties of long Josephson junctions have been studied in relation to their possible application in tuneable resonators [8]. On the other hand, driving long junctions by microwaves is now successfully used for phase-locking of Josephson flux-flow oscillators in integrated superconducting submillimeter wave receivers [9].

In this paper, we investigate experimentally (Section II) and numerically (Section III) the effect of microwave irradiation on *long* underdamped Josephson junctions. In particular, we are interested in the influence of microwaves on the current-voltage characteristics of the junctions at zero (or small) dc magnetic field. Our

*Permanent address: Institute of Solid State Physics, Chernogolovka, Moscow Region, 142432, Russia
†Present address: Theoretische Physik III, Ruhr-Universität Bochum, D-44801 Bochum, Germany

results suggest an explanation for previously observed microwave-induced smooth branches in I-V characteristics of intrinsic high-T_c junctions. We find that these smooth branches are due to flux flow, but the vortex motion is very irregular and shows spatially-temporal chaotic behavior.

It is interesting to note that the smooth branches in the I-V curves of long junctions resemble the ones observed in extremely small Josephson junctions driven by microwaves of a small frequency in the presence of large thermal fluctuations [10]. In this case the effect of microwaves on the I-V curves has been explained as incoherent multi-photon absorption in the Josephson phase diffusion regime. Thus, we will discuss (Section IV) our results by exploiting the analogy between the spatially-temporal chaos of vortex motion in long junctions and the diffusive behavior of the Josephson induced by thermal fluctuations in small Josephson junctions.

II. EXPERIMENTS

We performed measurements using Nb/Al-AlO$_x$/Nb long Josephson junctions [11] of overlap geometry. Below we present our results for the junction of the length $L = 250\,\mu$m and width $w = 3.5\,\mu$m. The critical current density j_c is about 180 A/cm^2, which corresponds to the Josephson penetration length λ_J of about 28 μm and zero-bias plasma frequency of $f_p \approx 77$ GHz. The sample was placed inside the vacuum volume of a variable-temperature optical cryostat. Magnetic field was applied in the plane of the junction perpendicular to its larger dimension. The dc measurements were carried out using a four-probe configuration.

We investigated the junction behavior under the microwave irradiation of a frequency in the range from 10 GHz to 20 GHz at two different temperatures 4.2 K and 5.0 K. The external microwave radiation was applied to the junction by an antenna placed outside the cryostat close to the optical window facing the sample. Thus, the ac bias current was induced by the antenna in the bias leads and across the junction. The typical power P of the applied microwave radiation was ranging from few pW to several mW, as referenced to the output port of the microwave source. Below we present and discuss the results obtained for the frequency of microwave radiation $f \equiv \omega/(2\pi) = 16.61$ GHz, which corresponds to the $f \simeq 0.2 f_p$. We note that results obtained at different frequencies within the studied range were qualitatively similar.

The dependence of the critical current of the junction on microwave power at zero magnetic field and temperature 4.2 K is shown in Fig. 1(a). The critical current I_c monotonically decreases with power and drops abruptly to zero at the power level $P_{cr} \approx 3$ dBm. This kind of behavior can be interpreted in general terms for nonlinear systems as a threshold in energy transmission [12]. For a long Josephson junction, it can be

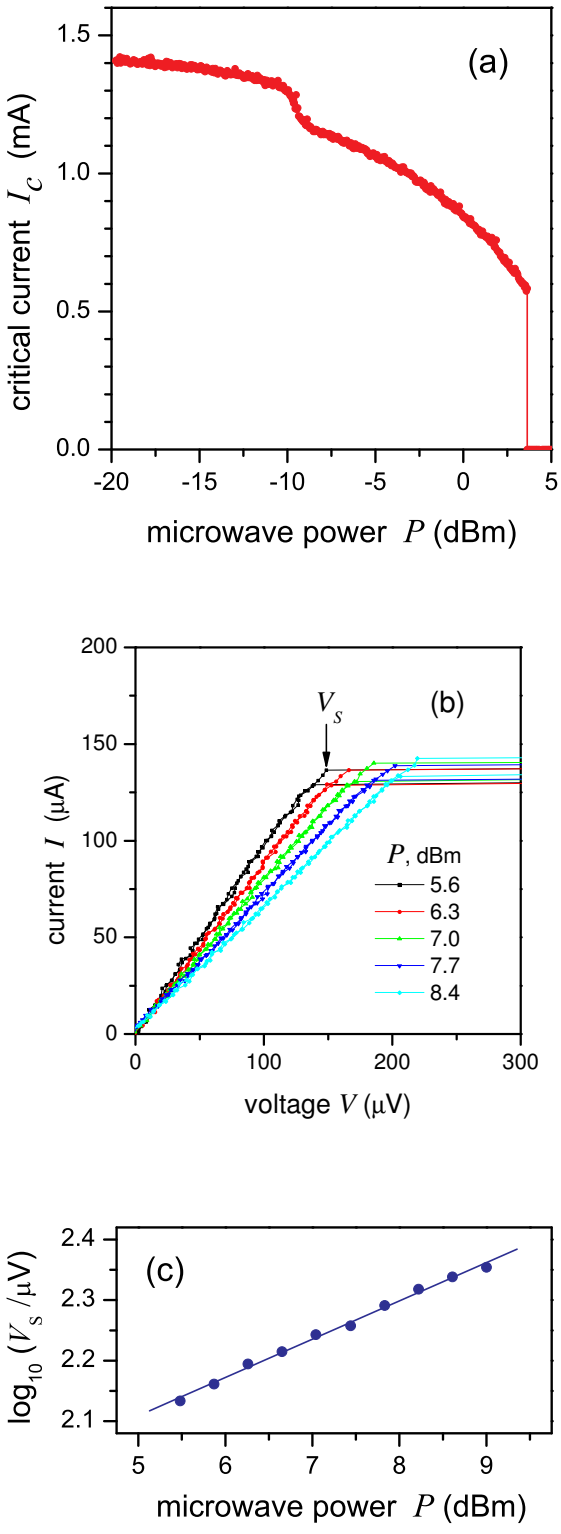

FIG. 1: (a) Critical current I_c of the junction at zero magnetic field versus the applied microwave power P at the frequency $f = 16.61$ GHz. (b) I-V curves for different power levels at $P > P_{cr}$. The measured voltage V_s at the top of the first curve is also shown. (c) Dependence of the voltage V_s on the microwave power P using double-logarithmic scale.

treated as ac-driven dissociation of a virtual breather (vortex-antivortex bound state) at the junction boundary [13]. A smoother drop occurs at the power level of $P_r \approx -10\,\mathrm{dBm}$. It is associated with the Josephson plasma resonance, which we will not address in the rest of the paper. Plasma resonance in long junctions has been studied previously in several experiments [14, 15].

As the applied microwave power exceeds P_{cr}, the supercurrent branch of the I-V curve disappears. Fig. 1(b) shows the gradual changes in I-V curves with increasing microwave power above P_{cr}. Each I-V curve has a linear region at low bias and its slope decreases with power. At a certain bias point, which depends on the power level, we observe a sudden jump from the voltage $V = V_s$ to much higher voltages of the energy gap at $V \approx 2.7\,\mathrm{mV}$. The dependence of the voltage V_s of this critical point on the applied power is presented in Fig. 1(c). We have found this dependence to be power-law $V_s \propto P^{\alpha}$ with the index $\alpha = 0.55 \pm 0.01$. Very similar behavior of the I-V curves was also observed at the temperature 5 K. The major difference was in the modified shape of the I-V curves, where the linear branch at low bias was replaced by a more pronounced pseudo-resonant feature, i.e. a peak with downward curvature. Figure 3(a) illustrates this behavior. The microwave power dependence of the switching voltage V_s (its position is marked in Fig. 3(a)) remained power-law with $\alpha = 0.62 \pm 0.01$.

It is worth mentioning that there is some uncertainty in determining the position of the switching voltage V_s (especially in the case of numerically calculated curves - see results below). At the same time, it will be useful in the following to have a criterion for the voltage which characterizes the effect of microwaves on the I-V curves. One could, for example, choose some current value and observe how the voltage V_I at this current changes with microwave power P. In such a case, however, question arises whether the behavior of $V_I(P)$ is universal or depends on current. We have investigated $V_I(P)$ dependence for three current values marked by dotted horizontal lines in Fig. 3(a). The dependence is always power-law $V_I \propto P^{\beta}$ at $\beta = 0.68$, 0.63 and 0.47 for current values 150; 184 and 223 μA correspondingly. Thus, the power-law $V \propto P^{x}$, where V is either V_s or V_I and value of x is close to 0.5, describes the IV-curve evolution versus applied microwave power with a reasonable accuracy.

It is interesting that the I-V curves under the influence of microwave irradiation resemble the well known flux-flow state of long Josephson junctions. The microwave field $\sqrt{P}$ affects the junction similarly to dc magnetic field H applied in the plane of the tunnel barrier. However, the sudden drop of the junction critical current I_c to zero at $P = P_{cr}$ qualitatively differs from behavior of I_c in dc magnetic field.

In order to experimentally obtain information about the microwave-induced vortex motion in the junction we have performed spatially-resolved measurements using a low-temperature Laser Scanning Microscope (LSM).

The principle of probing the junction by laser beam is to introduce a local heating of the sample at the beam position and to get the information about the local properties of the junction at this point. We scanned a focused laser beam over the junction area and simultaneously recorded its electrical response. The voltage response of a current-biased junction is due to the change of damping induced by local temperature increase at the illuminated spot. In order to improve the signal-to noise ratio and increase spatial resolution, the beam intensity is modulated at a frequency f_{mod} and the circuit response is detected using lock-in technique. The spatial resolution of this technique is limited by both the thermal healing length (depending on the material properties and f_{mod}) and the laser beam diameter. In the presented experiment it was about 2 μm.

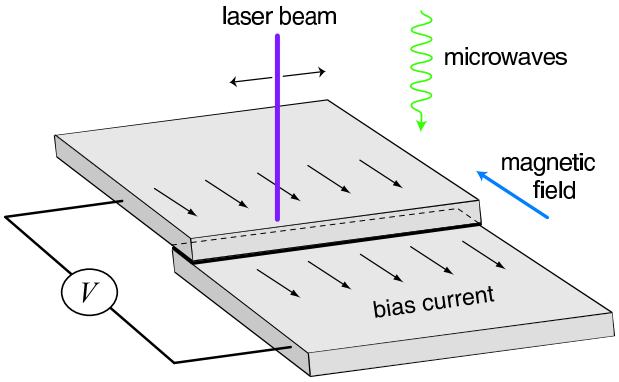

FIG. 2: Schematic view of the laser scanning experiment. Dimensions are not to scale.

Figure 2 illustrates the scheme of the LSM experiment. The junction area is scanned by tightly-focused laser beam, which power is modulated at $f_{\mathrm{mod}} = 100\,\mathrm{kHz}$. The voltage response δV arising due to the temperature oscillations is detected by lock-in technique. The characteristic time of a laser beam displacement is much longer than $1/f_{\mathrm{mod}}$, which allows to measure the voltage response for every geometrical point of the junction averaged over many thermal cycles. In its turn, the characteristic modulation time $1/f_{\mathrm{mod}}$ is much longer than the flux-flow oscillation frequency V/Φ_0 in the junction, where $\Phi_0 = h/(2e)$ is the magnetic flux quantum. We adjusted the laser beam power to have the relative magnitude of the voltage signal $|\Delta V/V| \simeq 10^{-3}$, which ensured that the beam acts as a weak perturbation of the dynamical state of the junction. In order to reduce noise, we averaged the measured δV over the junction width. We plot the inverted voltage response $(-\delta V)$ as a function of the laser beam position along the length of the junction.

Results of the LSM investigation of the junction state corresponding to point A marked on the I-V curve in Fig. 3(a) are presented in Fig. 3(b). The vertical axis displays the inverted voltage signal $(-\delta V)$ in arbitrary units. Solid circles illustrate the LSM response in the absence of dc external magnetic field. There is hardly

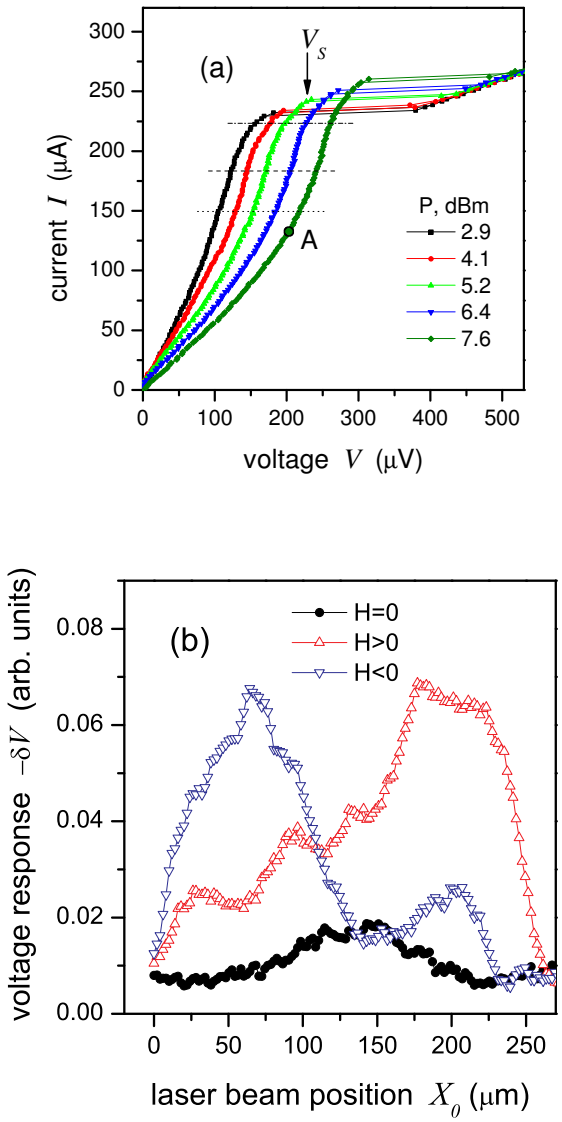

FIG. 3: (a) I-V curves for different power levels obtained at the same regime as ones from Fig. 1(b) but at higher temperature $T = 5\,\mathrm{K}$; (b) LSM response of the junction in a state corresponding to the marked bias point A in (a), at zero (solid circles) and non-zero dc magnetic fields ($H = 2.3\,\mathrm{Oe}$ up triangles, $H = -2.3\,\mathrm{Oe}$ down triangles).

any voltage response at the junction edges, while a noticeable maximum occurs in the center of the junction. The pattern is rather symmetric reflecting the symmetry of the junction at zero magnetic field.

To check the above hypothesis of the flux-flow nature of the observed microwave driven behavior of the junction, we also measured LSM patterns at non-zero dc magnetic field directed perpendicular to both current flow direction and junction length as shown in Fig. 2. The main idea of applying dc field is to break the symmetry between two junction edges and facilitate injection of Josephson vortices at one of them. We would expect that under such conditions the vortices would be mainly entering the junction from one edge. The measured response patterns corresponding to two magnetic fields of 2.3 Oe equal in magnitude but opposite in polarity are presented in Fig. 3(b) by up- and down-triangles. We clearly observe asymmetric patterns: For $H > 0$ a maximum of the response is located at the right half of the junction while in the case of $H < 0$ the maximum is shifted to the opposite junction edge. We obtained similar asymmetric patterns in non-zero magnetic field for all measured bias points of I-V curves in the Fig. 3(a), as well as for bias points in Fig. 1(b). The maximum in the voltage response $-\delta V$ was shifting back and forth between junction edges, depending on the polarity of the applied field. This fact indicates that the response is most probably generated by Josephson vortices entering the junction from one of the edges.

We note that similar asymmetric response patterns were observed for a pure flux-flow state in a long Josephson junction by Quenter et al. [16] and analyzed in Ref. [17]. The response is typically the largest in the region where vortices are injected in the junction. In detail, the effect of a local perturbation induced by a hot spot (e.g., laser beam) on vortex dynamics in the junction has been studied elsewhere [20].

Thus, we argue that junction dynamics under the microwave irradiation at relatively low frequency $f \ll f_p$ is governed by the injection of Josephson vortices at the junction edges. This hypothesis is further supported by numerical simulations presented in the following section.

III. NUMERICAL RESULTS

The ac-driven weakly damped long Josephson junction is described by the well-known perturbed sine-Gordon equation for the Josephson phase difference $\varphi(x,t)$

$$\varphi_{xx} - \varphi_{tt} - \sin\varphi = \alpha(x)\varphi_t - \gamma - \gamma_{\mathrm{ac}}\sin(\omega t)\,, \qquad (1)$$

where the subscripts stand for the partial derivatives, the coordinate x, running along the junction, and the time t are normalized so that the Josephson penetration length λ_{J} and plasma frequency $\omega_{\mathrm{p}} = 2\pi f_{\mathrm{p}}$ are both equal to unity. A parameter $\alpha(x)$ is the damping coefficient, which we will assume to be spatially dependent when simulating the effect of the laser beam on the junction. The term γ is the uniform bias current density normalized to the critical current density j_c, and γ_{ac} is the amplitude of uniformly-flowing ac current normalized in the same way.

If the long junction is placed in external dc and ac magnetic field, Eq. (1) is accompanied by the boundary conditions:

$$\varphi_x(0,t) \;=\; h - h_{\mathrm{ac}}\sin(\omega t), \qquad (2)$$

$$\varphi_x(\ell,t) \;=\; h + h_{\rm ac}\sin(\omega t), \qquad (3)$$

where $\ell = L/\lambda_{\rm J}$ is the normalized length of the junction. In (2) and (3) we take opposite signs in front of $h_{\rm ac}$ assuming that a part of ac bias (due to its nonuniform distribution) flows near the junction edges [18, 19]. The precise distribution of the oscillatory currents and fields induced by microwaves in the junction can be rather complex. We suppose that in the absence of a ground plane the largest microwave current is induced near the junction edges. That can be described by a distribution of the current $\gamma_{\rm ac}$ sharply peaked near the junction boundaries [8] or, equivalently, by an oscillating bias component $\pm\, h_{\rm ac}$ at the edges. In the following we show the simulation results obtained for $\gamma_{\rm ac} = 0$, so that microwave drive is coupled via the boundary conditions. We have also done simulations with a uniformly distributed $\gamma_{\rm ac}$ current and got qualitatively similar results.

We numerically integrated Eq. (1) with boundary conditions (2) and (3). The details of the simulation procedure can be found elsewhere [20]. Simulations were performed with parameters very close to our experiment described above: a normalized junction length $\ell = 8.9$, the normalized ac-drive frequency $\omega/(2\pi) = 0.2$, and two values of dissipation coefficient $\alpha(x) = \alpha_0 = 0.05$ and $\alpha_0 = 0.02$. The calculated averaged voltage Θ is just $\langle\dot\varphi\rangle$ normalized to the voltage at the first zero-field step (ZFS1) $\langle\dot\varphi\rangle_{\rm ZFS1} = 2\pi/\ell$.

Figure 4(a,b) shows the numerically calculated current-voltage characteristic for several values of the normalized ac field amplitude $h_{\rm ac}$ at zero dc magnetic field $h = 0$. As the amplitude of ac drive $h_{\rm ac}$ approaches the amplitude $h_{\rm ac} = 2$, the critical current is reduced and the I-V curves display a smooth branch at low voltages. In this regime, in order to obtain accurate enough curves we had to perform numerical integration over 40,000 time units at every bias point. Increasing the amplitude $h_{\rm ac}$ shifts the smooth branch towards high voltages. In some current ranges we observe locking of the I-V curves to vertical Shapiro steps at constant voltage. Figures 4(a) and 4(b) correspond to two different damping constants $\alpha_0 = 0.05$ and $\alpha_0 = 0.02$, respectively.

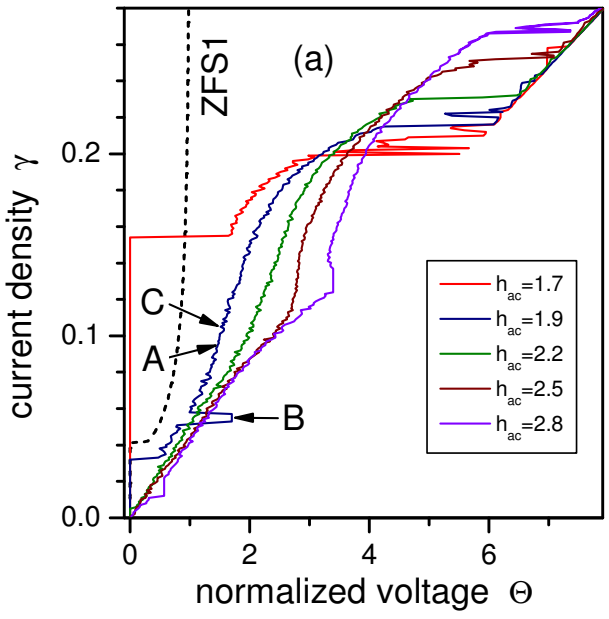

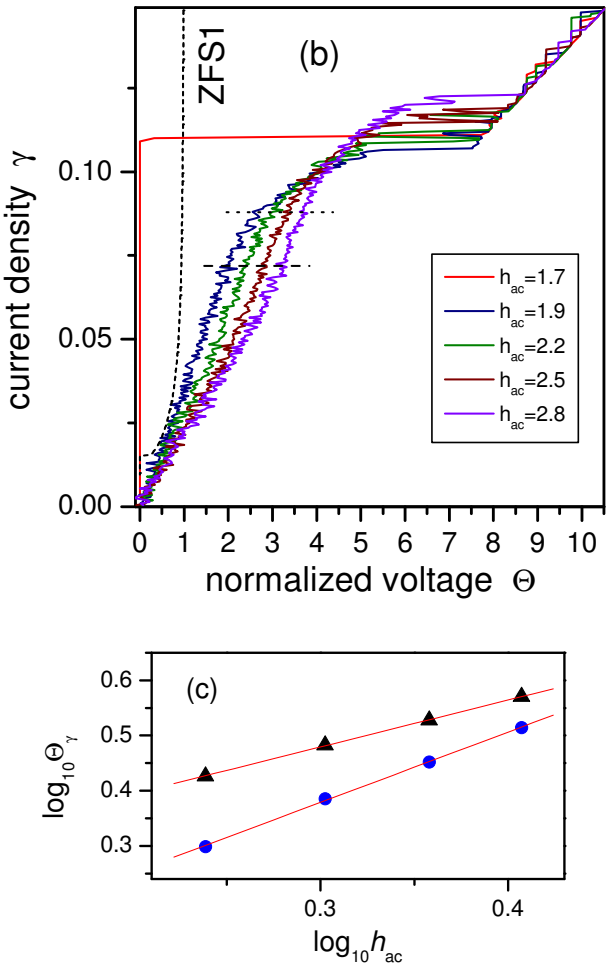

FIG. 4: Numerically calculated I-V curves for different amplitudes of the ac bias and two different values of dissipation: (a) $\alpha_0 = 0.05$; (b) $\alpha_0 = 0.02$. Dashed IV-curve shows the first zero-field step (ZFS1) corresponding to a vortex shuttling between junction boundaries in the absence of microwaves. (c) Dependence of the voltage Θ_γ at the dc bias levels $\gamma = 0.072$ (circles) and $\gamma = 0.088$ (triangles) indicated by horizontal dotted lines in (b) on ac-drive amplitude $h_{\rm ac}$ using double-logarithmic scale.

The dependence of the voltage Θ_γ taken at the constant dc bias levels $\gamma = 0.072$ and $\gamma = 0.088$ on the applied ac-drive amplitude $h_{\rm ac}$ is presented in Fig. 4(c). The best linear fits to the power law $\Theta_I \propto h_{\rm ac}^{\beta}$ are with the indices $\beta = 1.27\pm0.08$ and $\beta = 0.85\pm0.08$ for smaller and larger current values, correspondingly.

Thus, we find in good accord with the experimental results that the characteristic voltage values of the low volt-

age branch depend on the microwave power as $V \propto P^{1/2}$ (see Fig. 4(c)). By analogy with the flux-flow behavior, we argue that the characteristic voltage V is proportional to the average number of fluxons in the junction, which in its turn is roughly proportional to the microwave field intensity $\sim P^{1/2}$. We should take here into account that the microwave current generates magnetic field at the junction boundaries. At every time moment, the generated magnetic field components at the two long junction boundaries are equal in magnitude but opposite in polarity. If the field amplitude is larger than critical, there will be vortices injected at one junction boundary and antivortices injected at the other boundary. At microwave frequencies $f \ll f_p$ the magnetic field generated at the junction boundaries varies relatively slow in comparison with the vortex injection rate. Thus, at each junction boundary, there will be a bunch of vortices injected every half-period of microwave field and a bunch of antivortices injected at every other half-period. During half-period of the microwave oscillation, vortices on one side of the junction and antivortices on its other side are injected simultaneously and propagate through the junction under the influence of the dc bias current. Vortices and antivortices will eventually annihilate in the middle of the junction or, as the dissipation is rather low, may propagate through one another and annihilate at the opposite junction boundary.

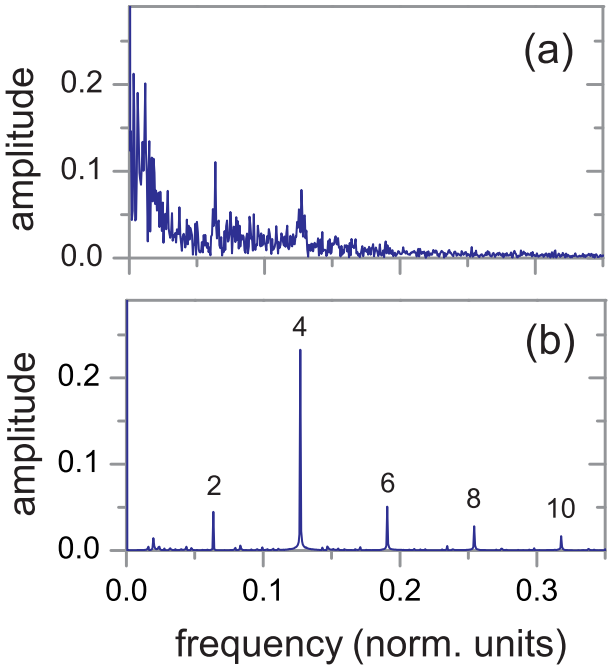

FIG. 5: Calculated voltage spectra at two bias points of the current-voltage curves shown in Fig. 4: (a) point A; (b) point B. The numbers near the peaks indicate the corresponding harmonics of the ac drive frequency.

We found that voltage oscillations in the junction are very *irregular* at nearly any point of smooth I-V branches. We calculated the Fourier power spectra of the voltage oscillations $\dot{\varphi}(t)$ at the center of the junction using FFT. Figure 5 illustrates such spectra for two points A and B of the current-voltage characteristics shown in Fig. 4(a). Point A displays a typical spectrum for the states along the smooth branches (see Figure 5(a)). Voltage oscillations are strongly irregular, the oscillation spectrum is very broad and resembles a chaotic state. Point B has been chosen at a Shapiro step, which is expected to be synchronized with the frequency of ac drive $f = \omega/(2\pi) \approx 0.0318$. In the corresponding spectrum presented in Fig. 5(b) we clearly see strong peaks at frequencies corresponding to various harmonics of the driving frequency. We suppose that the prevailing even harmonics are related to symmetric injection of vortices and antivortices into the junction from two boundaries.

Next we turn to a numerical simulation of our LSM experiment where the laser beam produces a local heating of the junction around the beam position at $x = x_0$. Thereby the dissipative term α is locally increased. We model the laser beam perturbation by a dissipative spot placed at the point $x = x_0$ and described by the following function:

$$\alpha(x) = \alpha_0 \left[1 + \varepsilon\delta(x - x_0)\right] . \qquad (4)$$

In simulations, we approximate the $\delta-$function by the expression [20]

$$\varepsilon\delta(x - x_0) \approx \kappa \left[1 - \tanh^2 \frac{2(x - x_0)}{\eta}\right] , \qquad (5)$$

where $\varepsilon = \kappa\eta$. In order to model the laser beam scanning procedure we calculate the time averaged voltage across the Josephson junction as a function of x_0 . This algorithm accounts for the experimental situation since the period of the fluxon oscillations is much shorter than the characteristic times of scanning and power modulation of the laser beam. Similarly to the experiment, the LSM patterns are presented in form of the dependence of the inverted voltage change $-\Delta\Theta(x_0)$ at a fixed bias point on the I-V curve. In simulations we have chosen the strength of the laser spot given by $\kappa = 2$ $\eta = 1$.

Figure 6 shows the calculated voltage response $-\Delta\Theta(x_0)$ obtained for the bias point C marked in Fig. 4. The scan shown by solid circles has been simulated at $h = 0$. Two types of triangles show simulation results for positive and negative dc magnetic field. These plots should be compared to experimentally measured ones presented in Fig. 3(b). One can see that simulations qualitatively match the experiment. In both cases, the response increases with the magnitude of magnetic field and becomes asymmetric. Inverting the field reverses the response with respect to the center of the junction. The magnetic field makes it favorable for vortices (or antivortices for negative fields) to enter from one boundary of the junction. The response is the largest near the boundary [16, 17], i.e. in the region where vortices enter the junction.

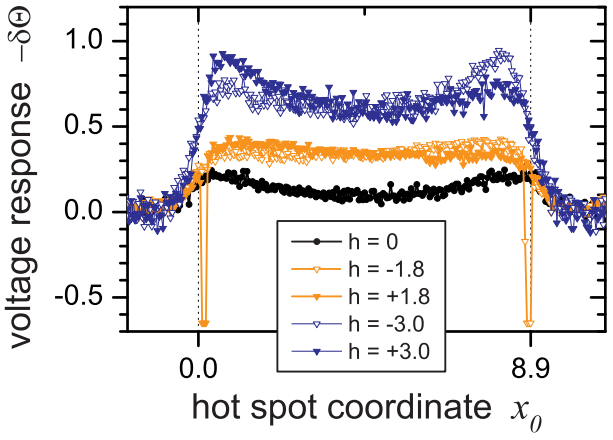

FIG. 6: Simulated LSM response of the junction in a state corresponding to the marked bias point C in Fig. 4(a), at zero (solid circles) and non-zero dc magnetic field (solid triangles for positive fields and open triangles for negative fields).

IV. DISCUSSION AND CONCLUSIONS

Our numerical studies show that applying of a microwave radiation of large amplitude induces a vortex flow in long Josephson junctions. As the frequency of ac drive is small, i. e. $f \ll f_p$, the dynamics of vortices is extremely irregular. It is appropriate to note here that chaotic dynamics in long junctions driven by ac field has been observed and discussed before [6]. However, the novelty of our results is in the particular appearance of the chaotic states in I-V curves, which we relate to experimental observations. Indeed, the observed low-voltage branches are similar to the well-known displaced linear branch, which is associated with chaotic dynamics in the absence of microwaves [7]. In both cases, the smooth branches shift towards high voltages with increasing the amplitude of the field (either ac or dc). This feature becomes even more pronounced, displaying the downward curvature (see Figs. 3(a) and 4(a)) as the chaos in vortex dynamics is reduced. Note here that the increase of temperature (and thus increase of dissipation) suppresses the chaos.

The presence of strong irregularities in the vortex motion allows us to draw an analogy with the properties of extremely small Josephson junctions subject to microwave radiation in the presence of large thermal fluctuations [10]. Indeed, in this case smooth low voltage branches in the I-V curve have been observed, and these branches also shift towards larger voltages proportionally to $\sqrt{P}$. This effect has been explained as an incoherent multi-photon absorption by the Josephson phase described by the diffusive motion induced by thermal noise. In this case we can write the lumped Josephson phase as

$$\varphi(t) \;=\; Vt + \psi(t) - \frac{\eta}{\alpha}\cos\omega t + \varphi_1(t) \quad , \qquad (6)$$

where η is the amplitude of ac drive, the random function

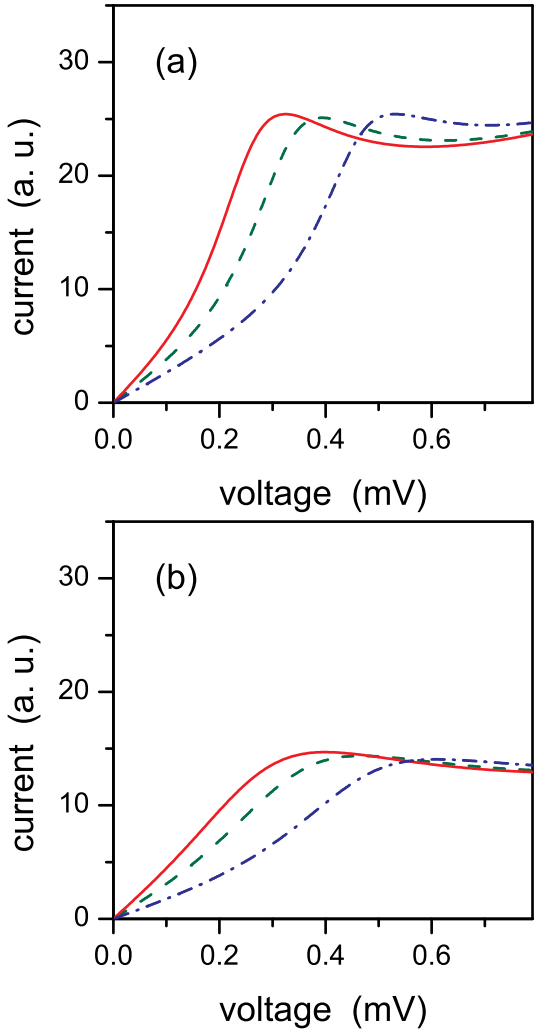

FIG. 7: The power dependence of I-V curves calculated using Eq. (7) for two values of parameter δ: (a) $\delta = 0.0001$; (b) $\delta = 0.0002$. The power levels correspond to $P = 2,\ 5,\ 7$ dBm. In both cases the linear slope corresponding to quasiparticle resistance $R = 50$ kΩ (a) and $R = 140$ kΩ (b), is added.

$\psi(t)$ determines the Josephson phase diffusion, and $\varphi_1(t)$ has to be found self-consistently [10]. As the frequency ω is small, we have obtained the low voltage branch of I-V curve in the following analytical form:

$$I_s(V) = I_c\frac{1}{2\alpha}[f_+(V-V_s)f_+(V+V_s) - f_-(V-V_s)f_-(V+V_s)] \ , \qquad (7)$$

where the functions $f_\pm(x) = \frac{\sqrt{\sqrt{x^2+\delta^2}\pm x}}{\sqrt{x^2+\delta^2}}$. Here, the maximum voltage of the branch $V_s = \eta/\alpha \propto \sqrt{P}$, and δ is the parameter characterizing the strength of fluctuations. The I-V curves are presented in Fig. 7 for different values of microwave power and two values of δ. Note here, that the low voltage branch appears in the limit of $\omega \ll \delta$ as the thermal fluctuations wash out the Shapiro steps. As the fluctuations characterized by the parameter δ increase, the I-V curve gets more linear (see

Fig. 7(b)).

We see that all features obtained for microwave induced irregular vortex flow in long junctions resemble ones observed in a small microwave driven Josephson junction in the presence of thermal fluctuations. Thus we argue that the ansatz (6) can be qualitatively used in the case of a microwave induced vortex flow, where the random function $\psi(t)$ is due to chaos in vortex motion. The chaos in the vortex motion mimics thermal fluctuations and wash out the I-V curve. According to both our experiment and numerical study, the reduction of chaos by increasing the damping (i. e. decreasing δ) leads to the pseudo-resonant feature on the I-V curve (see Figs. 3(a) and 4(a)). It is interesting to note that an increase of temperature (dissipation) in the case of long Josephson junction leads to *smaller* chaos-induced fluctuations. This is opposite to the case of a small Josephson junctions where the parameter δ increases with an increase of temperature.

In summary, we reported here experimental and numerical study of microwave-induced effects on the current-voltage characteristics of long Josephson junctions. We observed that low-frequency microwaves act on the junction I-V curves similar to the effect of dc magnetic field, i.e. induce the flux-flow behavior. Experiments using a low-temperature laser scanning microscope unambiguously indicate the motion of Josephson vortices driven by microwaves. Numerical simulations are in a good agreement with experimental data and indicate that the vortex flow is strongly irregular. Our results provide also an explanation for previously measured I-V curves of intrinsic high-T_c Josephson junctions driven by microwaves [3].

When this work was completed, we also learned about recent numerical data of the Tuebingen group [21]. Their simulations using the stacked junction model with the parameters of intrinsic junctions also show chaotic regimes in the vortex dynamics driven by microwaves, which is consistent with our observations.

Acknowledgements

We are indebted to R. Kleiner and H.B. Wang for valuable discussions.

[1] R. Kleiner, F. Steinmeyer, G. Kunkel, and P. Müller, Phys. Rev. Lett. **68**, 2394 (1992); R. Kleiner and P. Müller, *Phys. Rev. B* **49**, 1327 (1994).

[2] O.K.C. Tsui, N.P. Ong, Y. Matsuda, Y.F. Yan, and J.B. Peterson, Phys. Rev. Lett. 73, 724 (1994); Y. Matsuda, M.B. Gaifullin, K. Kumagai, K. Kadowaki and T. Mochiku, Phys. Rev. Lett. **75**, 4512 (1995); L.N. Bulaevskii; M.P. Maley, and M. Tachiki, Phys. Rev. Lett. **74**, 801 (1995); A.E. Koshelev, Phys. Rev. Lett. **77**, 3901 (1996).

[3] A. Irie and G. Oya, IEEE Trans. Appl. Supercond. **5**, 3267 (1995); Yu.I. Latyshev, P. Monceau, and V.N. Pavlenko, Physica C **293**, 174 (1997); W. Prusseit, M. Rapp, K. Hirata, and T. Mochiku, Physica C **293**, 25 (1997); H.B. Wang, Y. Aruga, T. Tachiki, Y. Mizugaki, J. Chen, K. Nakajima, T. Yamashita, and P.H. Wu, Appl. Phys. Lett. **74**, 3693 (1999); Y.J. Doh, J.H. Kim, H.S. Chang, S.H. Chang, H.J. Lee, K.T. Kim, W. Lee, and J.H. Choy, Phys. Rev. B **63**, 144523 (2001).

[4] G. Costabile, R. Monaco, S. Pagano, and G. Rotoli, Phys. Rev. B **42**, 2651 (1990).

[5] M. Salerno, M. R. Samuelsen, G. Filatrella, S. Pagano, and R. D. Parmentier, Phys. Rev. B **41**, 6641 (1990); N. F. Pedersen and A. Davidson, Phys. Rev. B **41**, 178 (1990); N. Grønbech-Jensen, Phys. Rev. B **47**, 5504 (1993); N. Grønbech-Jensen and M. Cirillo, Phys. Rev. B **50**, 12851 (1994); M. Cirillo, P. Cocciolo, V. Merlo, N. Grønbech-Jensen, and R. D. Parmentier, J. Appl. Phys. **75**, 2125 (1994).

[6] M. Cirillo, J. Appl. Phys. **60**, 338 (1986); M. Cirillo, A.R. Bishop, N. Grønbech-Jensen and P.S. Lomdahl, Phys. Rev. E **49**, 3606 (1994).

[7] A. V. Ustinov, H. Kohlstedt, and P. Henne, Phys. Rev. Lett. **77**, 3617 (1997); M. Cirillo, T. Doderer, S. G. Lachenmann, F. Santucci, and N. Grønbech-Jensen, Phys. Rev. B **56**, 11889 (1997).

[8] E. Goldobin, A.M. Klushin, M. Siegel, and N. Klein, J. Appl. Phys. **92**, 3239 (2002).

[9] V.P. Koshelets and S.V. Shitov, Supercond. Sci. Technol. **13**, R53 (2000).

[10] Y. Koval, M. V. Fistul and A. V. Ustinov, submitted to Phys. Rev. Lett. (2004).

[11] The sample was fabricated using our layout at the foundry of IPHT Jena, Germany (*http://www.ipht-jena.de*).

[12] F. Geniet and J. Leon, Phys. Rev. Lett. **89**, 134102 (2002).

[13] M. V. Fistul, B. A. Malomed, and A. V. Ustinov (unpublished).

[14] M. Cirillo, G. Costabile, S. Pace, and B. Savo, IEEE Trans. Magn. **19**, 1014 (1983); T. Holst and J. Bindslev Hansen, Phys. Rev. B **44**, 2238 (1991); M.V. Fistul and A.V. Ustinov, Phys. Rev. B **63**, 024508 (2001);

[15] N.F. Pedersen and S. Sakai, Phys. Rev. B **58**, 2820 (1998); S. Sakai and N.F. Pedersen, Phys. Rev. B **60**, 9810 (1999).

[16] D. Quenter, A. V. Ustinov, S. G. Lachenmann, T. Doderer, R. P. Huebener, F. Müller, J. Niemeyer, R. Pöpel, and T. Weimann, Phys. Rev. B **51**, 6542 (1995).

[17] M. V. Fistul and A. V. Ustinov, Inst. Phys. Conf. Ser, **167**, 177 (2000).

[18] O. H. Olsen and M. R. Samuelsen, J. Appl. Phys. **54**, 6522 (1983).

[19] M. R. Samuelsen and S. A. Vasenko, J. Appl. Phys. **57**, 110 (1985).

[20] B. A. Malomed and A. V. Ustinov, Phys. Rev. B **49**, 13024 (1994).

[21] T. Clauss, T. Uchida, M. Mößle, D. Koelle, and R.

Kleiner (unpublished).